

Multifunctional Linear Triferrocene Derivatives Linked by Oxidizable Bridges: Optical, Electronic, and Cation Sensing Properties

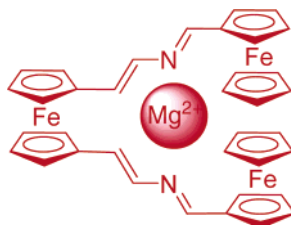
Antonio Caballero, Alberto Tárraga,* María D. Velasco, Arturo Espinosa, and Pedro Molina*

Departamento de Química Orgánica, Universidad de Murcia,
Campus de Espinardo, 30071 Murcia, Spain

pmolina@um.es

Received April 15, 2005

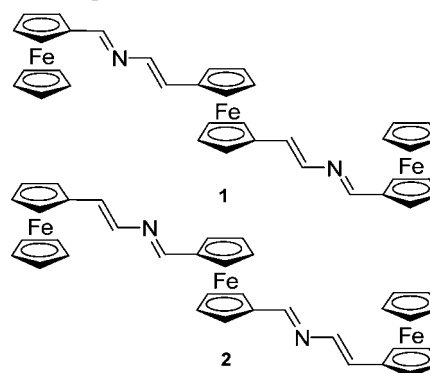
ABSTRACT



A novel linear triferrocene derivative has been prepared and proven to be of special interest in the study of intramolecular electron transfer and as a specific optical and electrosensor for Mg^{2+} cation.

Recently, oligomeric ferrocene-based species have attracted attention with respect to their electrochemical, electronic, and magnetic properties.¹ Although there are numerous studies on bridged biferrocene systems, reports on trinuclear ferrocene derivatives are considerably less frequent and only very few electrochemical studies have been published on linear bridged triferrocenes.² We report here the synthesis, characterization, and properties of a new type of homotrimetallic π -conjugated complexes **1** and **2** (Scheme 1) in which the ferrocenyl subunits are both linearly linked by two oxidizable 2-aza-diene bridges, which additionally comprise putative cation-binding sites, and in close enough proximity to permit redox coupling.

Scheme 1. Preparation of Triferrocene Derivatives **1** and **2**



Compounds **1** and **2** were prepared from the readily available diethyl aminomethylphosphonate,³ following the

(1) Barlow, S.; O'Hare, D. *Chem. Rev.* **1997**, 97, 637.
(2) (a) Pannell, K. H.; Dementiev, V. V.; Li, H.; Cervantes-Lee, F.; Nguyen, M. T.; Diaz, A. F. *Organometallics* **1994**, 13, 3644. (b) Barlow, S.; Murphy, V. J.; Evans, J. S. O.; O'Hare, D. *Organometallics* **1995**, 14, 3461. (c) Rulkens, R.; Lough, A. J.; Manners, I.; Lovelace, S. R.; Grant, C.; Geiger, W. E. *J. Am. Chem. Soc.* **1996**, 118, 12683. (d) Hirao, T.; Kurashima, M.; Aramaki, K.; Nishihara, H. *J. Chem. Soc., Dalton Trans.* **1996**, 2929. (e) Tárraga, A.; Molina, P.; Curiel, D.; Velasco, M. D. *Organometallics* **2001**, 20, 2145.

(3) Davidsen, S. K.; Phillips, G. W.; Martin, S. F. *Org. Synth.* **1993**, 8, 451.

recently described method for the synthesis of 1,4-disubstituted 2-aza-1,3-butadienes.⁴

Electrochemical studies and CV and DPV experiments revealed that compounds **1** and **2** show electroactivity due both to the presence of the ferrocenyl moieties and to the oxidation of the 2-aza-1,3-butadiene bridges. They show three oxidation waves in the range 0–1.5 V vs decamethylferrocene (DMFc): the first two waves correspond to two reversible oxidation processes and are assigned to the oxidation of the ferrocene subunits, while the third wave ($E_p = 1.120$ and 1.020 V, vs DMFc, respectively) is clearly irreversible and may be assigned to the oxidation of the bridge. The oxidation potentials of the ferrocenyl units are dependent on the position of the 2-aza-diene bridge to which they are attached: $E_{1/2} = 0.470$ V (one-electron oxidation) and 0.690 V (two-electron oxidation), vs DMFc, for the central and terminal ferrocenyl units in **1** and $E_{1/2} = 0.510$ V (two-electron oxidation) and 0.840 V (one-electron oxidation), vs DMFc, for the terminal and central ferrocenyl units in **2**, respectively (see the Supporting Information).

Spectrophotometric studies of these compounds were also carried out on both their neutral and chemically or electrochemically generated oxidized forms. The electronic absorption spectra of the neutral compounds show two prominent high energy (HE) absorption bands at 256–258 nm and 333–336 nm assigned to the π – π^* transitions mainly within the 2-aza-1,3-diene bridge. In addition to these bands, another weaker low energy (LE) absorption in the region 483–485 nm is assigned to a ferrocenyl-based metal-to-ligand (MLCT) band (see the Supporting Information).

Generation of the oxidized species derived from **1** and **2** was performed either by chemical oxidation with the appropriate amount of silver trifluoromethanesulfonate or by constant potential electrolysis, 0.12 V above $E_{1/2}$ of the first ferrocenyl redox couple (0.59 V for **1** and 0.63 V for **2**), and monitored by absorption spectroscopy (see the Supporting Information). During the oxidation of the central ferrocenyl subunit in **1** (0–1 range of removed electrons), a new LMCT (Cp–Fe(III)) band at $\lambda = 557$ nm ($\epsilon = 5722$ M^{−1} cm^{−1}) appears with concomitant decreasing of the band at $\lambda = 483$ nm ($\epsilon = 5263$ M^{−1} cm^{−1}) (Figure 1a). Moreover, in the NIR region a new band at $\lambda = 1296$ nm ($\epsilon = 140$ M^{−1} cm^{−1}) appears, increasing continuously its intensity until one electron is removed, and which is assigned to a bridge-mediated superexchange process between the two different coupled iron sites Fe(III) and Fe(II) (intervalence charge-transfer band: IVCT). Along with the changes of these bands, defined isosbestic points at $\lambda = 424$ nm and $\lambda = 509$ nm are maintained during the course of the oxidation process. Interestingly, on removing more electrons (from 1 to 3 at a constant potential of 0.81 V) the intensity of the band at $\lambda = 1296$ nm decreases until it disappears when the compound is fully oxidized, but at the same time, two new bands appear at $\lambda = 750$ nm ($\epsilon = 440$ M^{−1} cm^{−1}) and $\lambda = 1059$ nm ($\epsilon = 460$ M^{−1} cm^{−1}) which could be attributed to a 2-aza-diene to Fe(III) LMCT transitions (Figure 1b). Similar low energy

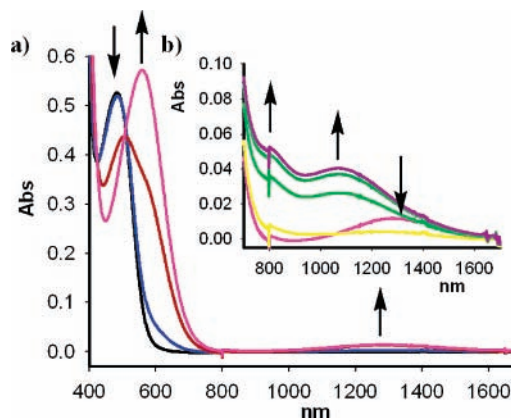


Figure 1. Evolution of vis-near-IR spectra during the oxidation of **1** ($c = 1 \times 10^{-3}$ M in CH₂Cl₂ with Bu₄NPF₆ (0.15 M) as supporting electrolyte) when (a) 0 (black), 0.2 (blue), 0.5 (red), and 1 (pink) electron is removed and (b) 1 (pink), 1.5 (yellow), 2 (green), 2.5 (deep green), and 3 (purple) electrons are removed.

transitions have also been observed in other aza-substituted ferrocenes which by electrochemical oxidation of the Fe(II) show the intramolecular electron-transfer between the N atom of the ligand and the Fe(III) centers.⁵

During the oxidation of **2** by continuous removal of a number of electrons between 0 and 2, the band in the visible region ($\lambda = 485$ nm) present in the neutral ligand progressively disappears, and at the same time, a new band at $\lambda = 577$ nm ($\epsilon = 6600$ M^{−1} cm^{−1}), which is assigned to a ligand-to-metal (LMCT) charge transfer, continuously increase in intensity, reaching a maximum when two electrons have been removed. Furthermore, defined isosbestic points at $\lambda = 450$ nm and $\lambda = 511$ nm are maintained during the course of the oxidation process (see the Supporting Information). On the other hand, the three bands at the near-IR, at $\lambda = 750$ nm ($\epsilon = 500$ M^{−1} cm^{−1}), $\lambda = 950$ nm ($\epsilon = 390$ M^{−1} cm^{−1}), and $\lambda = 1228$ nm ($\epsilon = 270$ M^{−1} cm^{−1}), not observed in the neutral ligand, present different behavior whereas the oxidation of the central ferrocenyl subunit is taking place (removal from 2 to 3 electrons, at a constant potential of 0.96 V). Thus, while the latter completely disappears during this process, the former, at $\lambda = 750$ nm and $\lambda = 950$ nm, increase continuously until the total oxidation is achieved (see the Supporting Information). These experimental facts suggest that the absorption bands at $\lambda = 750$ nm and $\lambda = 950$ nm could be due to a 2-aza-diene to Fe(III) LMCT transition while the band at $\lambda = 1228$ nm could be attributed to a bridge-mediated superexchange process between the two external Fe(III) and the central Fe(II) (IVCT band). It is worth noting that superexchange and hopping mechanisms can both contribute when an electron or hole is transferred from a donor to an acceptor with the assistance of an intermediate or “midway” group. Moreover, in the super-

(4) Caballero, A.; Tormos, R.; Espinosa, A.; Velasco, M. D.; Tárraga, A.; Miranda M. A.; Molina, P. *Org. Lett.* **2004**, *6*, 4599.

(5) (a) Horie, M.; Suzuki, Y.; Osakada, K. *J. Am. Chem. Soc.* **2004**, *126*, 3684. (b) Horie, M.; Sakano, T.; Osakada, K.; Nakao, H. *Organometallics* **2004**, *23*, 18.

exchange process, direct long-distance electron transfer is enhanced by indirect mixing of the donor and acceptor wave functions while in the hopping mechanism the charge is temporarily localized on the midway group and a chemical intermediate is produced.⁶

The spectral parameters of the bands present in the NIR, obtained by deconvolution of the experimental spectra performed on spectral intensity times wavenumber vs wavenumber assuming Gaussian shapes (see the Supporting Information), have been used to determine the effective electronic parameters V_{LM} and $V_{MM'}$, corresponding to the intramolecular electron-transfer phenomena (LMCT and IVCT) observed in the oxidized forms of these compounds by using the Hush's equation.⁷ An inspection of the resulting V_{ab} values shows that the electronic couplings between the ferrocenyl and 2-aza-1,3-butadiene bridge are moderate, so that these complexes belong to class II category.⁸ The relative values of V_{LM} (LMCT) ($131\text{--}663\text{ cm}^{-1}$) and $V_{MM'}$ (ICVT) ($99\text{--}150\text{ cm}^{-1}$) (see the Supporting Information) indicate that the intramolecular electron transfer (IET) may proceed through the two above-mentioned pathways.⁹

One of the most interesting attributes of ligands **1** and **2** is the presence of differentiated redox-active ferrocene moieties close to the cation-binding nitrogen atom. The metal recognition properties of ligands **1** and **2** were evaluated by optical, electrochemical and ^1H NMR techniques.

Due to the absorption phenomena observed on the electrode's surface, upon addition of metal cations, differential pulse voltammetry (DPV) was used to evaluate the binding ability of **1** and **2**. Then, whereas no perturbation of the DPV voltammogram of **1** was observed upon addition of Ca^{2+} ion, significant modifications could be observed upon addition of Mg^{2+} , although the evolution of the DPV was strongly dependent on the number of equivalents of the metal cation added. So, upon addition of 0–0.6 equiv of Mg^{2+} a clear evolution of the first oxidation peak, from $E_{1/2} = 0.470\text{ V}$ to $E_{1/2} = 0.670\text{ V}$, vs DMFc, was observed, while the second oxidation wave of the free ligand was apparently not perturbed during these additions. However, when larger amounts of Mg^{2+} (0.6–1 equiv) were added, a new wave at $E_{1/2} = 0.820\text{ V}$ vs DMFc appeared, which increases in intensity and reaches the maximum upon addition of 1 equiv of Mg^{2+} (Figure 2). These observations suggest that the first oxidation process of $\mathbf{1}\cdot\text{Mg}^{2+}$ ($E_{1/2} = 0.690\text{ V}$) practically

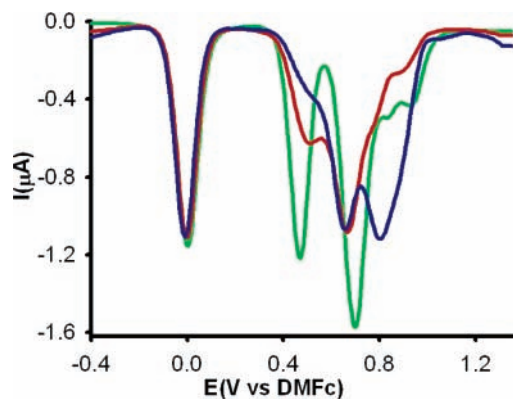


Figure 2. Evolution of the DPV of **1** (1 mM) in $\text{CH}_2\text{Cl}_2/[(n\text{-Bu})_4\text{N}]\text{ClO}_4$ scanned at 0.1 V s^{-1} from -0.7 V to 1.4 V when 0 (green), 0.6 (red), and 1 (blue) equiv of Mg^{2+} is added.

occurs at the same potential as that observed for the oxidation of the monooxidized ligand $\mathbf{1}^+$ ($E_{1/2} = 0.670\text{ V}$). Remarkably, the shift in redox potential of the complexed ($\mathbf{1}\cdot\text{Mg}^{2+}$) and neutral ligand ($\Delta E_{1/2} = 200\text{ mV}$) is the signature of a large value for the equilibrium constant for Mg^{2+} cation binding by the neutral receptor **1**,¹⁰ the binding enhancement factor (BEF) being 4.2×10^{-4} and the reaction coupling efficiency (RCE)¹¹ being 2402 (see the Supporting Information). In contrast, the lower value of the equilibrium constant for Mg^{2+} cation binding by the monooxidized ligand could explain the absence of the second oxidation wave at $E_{1/2} = 0.820\text{ V}$ ($\mathbf{1}^{2+}\cdot\text{Mg}^{2+}/\mathbf{1}^+\cdot\text{Mg}^{2+}$) when less than 0.8 equiv of Mg^{2+} was added.

On the other hand, the most significant features observed upon addition of $\text{Mg}(\text{ClO}_4)_2$ to an electrochemical solution of **2** can be summarized as follows: at the expense of the first oxidation peak at $E_{1/2} = 0.510\text{ V}$, vs DMFc, a new peak appears at $E_{1/2} = 0.630\text{ V}$, vs DMFc, associated with the oxidation of the terminal ferrocenyl units in the complexed form $\mathbf{2}\cdot\text{Mg}^{2+}$. Moreover, an analogous decrease in the intensity of the wave at $E_{1/2} = 0.840\text{ V}$ was also observed. The magnitude of the electrochemical shift ($\Delta E_{1/2} = 120\text{ mV}$) is also related to the complexation constant for this process, and the BEF and RCE were 9.4×10^{-3} and 107, respectively.

UV–vis spectroscopy was also used for the study of the complexation behavior of **1** and **2** because previous studies on ferrocene¹² ligands have shown that the characteristic band between 400 and 500 nm, ascribed to the lowest energy metal-to-ligand (MLCT) transition, is perturbed by complexation.¹³

(6) (a) Paulson, B. P.; Miller, J. R.; Gan, W.-X.; Closs, G. *J. Am. Chem. Soc.* **2005**, *127*, 4860. (b) Winters, M. U.; Pettersson, K.; Martensson, J.; Albinsson, B. *Chem. Eur. J.* **2005**, *11*, 562 and references therein.

(7) Hush, N. S. *Coord. Chem. Rev.* **1985**, *64*, 135.

(8) (a) Robin, M.; Day, P. *Adv. Inorg. Chem.* **1967**, *10*, 247. (b) Creutz, C. *Prog. Inorg. Chem.* **1983**, *30*, 1. Mixed-valence compounds are classified in three categories. Class I: the redox centers are completely localized and behave as separate entities. Class II: intermediate coupling between the mixed-valence centers exists. Class III: the system is completely delocalized and the redox centers show intermediate valence states.

(9) The presence of several NIR bands in the spectrum of a mixed-valence complex is not uncommon, and their occurrence is generally explained by means of three possible causes one of them being the presence of a bridge with accessible redox state levels: (a) Kober, E. M.; Goldby, K. A.; Narayand, D. N. S.; Meyer, T. J. *J. Am. Chem. Soc.* **1983**, *105*, 4303. (b) Lay, P. A.; Magnuson, R. H.; Taube, H. *Inorg. Chem.* **1988**, *27*, 2364. (c) Laidlaw, W. M.; Denning, R. G. *J. Chem. Soc., Dalton Trans.* **1994**, 1987. (d) Nelsen, S. F.; Ismagilov, R. F.; Powell, D. F. *J. Am. Chem. Soc.* **1998**, *120*, 1924.

(10) Miller, S. R.; Gustowski, D. A.; Chen, Z. H.; Gokel, G. W.; Echegoyen, L.; Kaifer, A. E. *Anal. Chem.* **1988**, *60*, 2021.

(11) (a) Beer, P. D.; Gale, P. A. *Adv. Phys. Org. Chem.* **1998**, *31*, 1. (b) Beer, P. D. *Acc. Chem. Res.* **1998**, *31*, 71. (c) Beer, P. D.; Gale, P. A.; Chen, G. Z. *Coord. Chem. Rev.* **1999**, 185–186, 3.

(12) (a) Marder, S. R.; Perry, J. W.; Tiemann, B. G. *Organometallics* **1991**, *10*, 1896. (b) Coe, B. J.; Jones, C. J.; McCleverty, J. A.; Bloor, D.; Cross, G. J. *J. Organomet. Chem.* **1994**, *464*, 225. (c) Lambert, C.; Gaschler, W.; Zabel, M.; Matschiner, R.; Wortmann, R. *J. Organomet. Chem.* **1999**, *592*, 109. (d) Müller, T. J.; Netz, A.; Ansorge, M. *Organometallics* **1999**, *18*, 5066.

Therefore, upon addition of a solution of anhydrous $\text{Mg}(\text{ClO}_4)_2$ in acetonitrile ($c = 2.5 \times 10^{-2} \text{ M}$) into a CH_2Cl_2 solution ($1 \times 10^{-4} \text{ M}$) of **1**, the MLCT band at $\lambda = 483 \text{ nm}$ ($\epsilon = 5190 \text{ M}^{-1} \text{ cm}^{-1}$) entirely disappeared and was replaced by a new band at $\lambda = 564 \text{ nm}$ ($\epsilon = 9750 \text{ M}^{-1} \text{ cm}^{-1}$) accompanied by an increase in absorbance (Figure 3a). Two

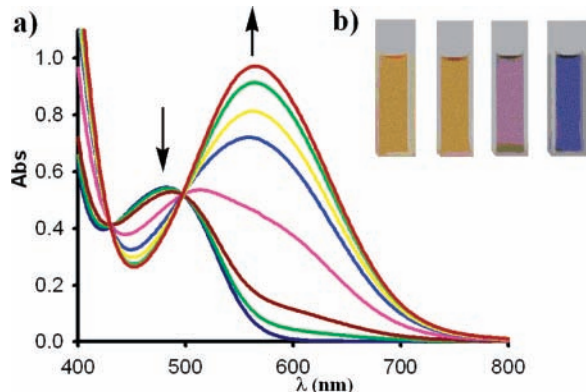


Figure 3. (a) Evolution of the UV-vis of **1**, upon addition of Mg^{2+} . (b) Evolution of the color in the CH_2Cl_2 solutions of **1** upon addition of Mg^{2+} : free ligand (left) and after addition of 0.33, 0.66, and 1 equiv of Mg^{2+} , respectively.

isosbestic points at $\lambda = 428$ and 500 nm were found, indicating the presence of a unique complex in equilibrium with the neutral ligand. The resulting titration isotherm fitted¹⁴ nicely a 1:1 binding model (see the Supporting Information) and the association constant was $1.02 \times 10^6 \text{ M}^{-1}$ (error < 10%). Preliminary theoretical calculations show that the $\mathbf{1} \cdot \text{Mg}(\text{ClO}_4)_2$ complex should be formed upon rotation of one-half of the otherwise centrosymmetric most stable conformation of **1** and of one azadiene bridge, so as both nitrogen electron pairs point in a convergent fashion to the inner triferrocene hinge cavity, to give a roughly lineal (152.0°) N–Mg–N array. Interestingly, upon addition of Mg^{2+} the color of the resulting solution changes from orange to purple which can be used for “naked eye” detection of Mg^{2+} (Figure 3b).

On the other hand, on titration of compound **2** under the same experimental conditions, the MLCT band at $\lambda = 485$

nm ($\epsilon = 6080 \text{ M}^{-1} \text{ cm}^{-1}$) completely disappeared and a new band red-shifted at $\lambda = 585 \text{ nm}$ ($\epsilon = 4770 \text{ M}^{-1} \text{ cm}^{-1}$) progressively appeared, although only an isosbestic point at $\lambda = 447 \text{ nm}$ was detected in this case (see the Supporting Information).

Moreover, ^1H NMR studies based on the titration of a CDCl_3 solution of **1** or **2** ($c = 1 \times 10^{-3} \text{ M}$) with Mg^{2+} showed that the spectra recorded after addition of increasing amounts of Mg^{2+} do not exhibit significant changes, as in the case of using ligand **2**. In contrast, addition of 1 equiv of Mg^{2+} to the ligand **1** gives rise to significant downfield shifts for the signals corresponding to the iminic proton ($\text{CH}=\text{N}$) at $\delta = 8.07 \text{ ppm}$ ($\Delta\delta = +0.28 \text{ ppm}$) as well as for the signals of the Cp protons appearing at $\delta = 4.69$ ($\Delta\delta = +0.12 \text{ ppm}$) and at $\delta = 4.44$ ($\Delta\delta = +0.30 \text{ ppm}$) together with a slight upfield shifts for the signals at $\delta = 6.99$ ($\text{CH}=\text{CH}-\text{N}$) ($\Delta\delta = -0.19 \text{ ppm}$) and $\delta = 6.58$ ($\text{CH}=\text{CH}-\text{N}$) ($\Delta\delta = -0.11 \text{ ppm}$) (see the Supporting Information). These results are in agreement with above-mentioned calculated (B3LYP/3-21G*) structure for $\mathbf{1} \cdot \text{Mg}(\text{ClO}_4)_2$ in which the nitrogen atoms within the azabutadiene bridges participate in the complexation process.

It is remarkable that upon addition of other metal ions such as Na^+ , K^+ , and Ca^{2+} , under the same conditions, no modification of either UV-vis or ^1H NMR spectra or voltammperograms of ligands **1** and **2** was observed with reference to those of the neutral ligands.

The triferrocene derivatives **1** presented here comprise a remarkable multifunctional molecular system. The presence of low energy bands in the partially oxidized forms indicates the existence of optical induced IETs between the iron centers and the organic bridges. The system has also shown to be an efficient dual-mode optical/electrochemical sensor for Mg^{2+} cations.

Acknowledgment. We gratefully acknowledge grants from DGI-Spain CTQ 2004-02201 and Fundación Séneca (CARM-Spain) PB/72/FS/02.

Supporting Information Available: General comments. Characterization data. CV and UV-vis of **1** and **2**. Preparation of the oxidized species and evolution of the vis-NIR of **2**. Deconvolution of NIR spectra. Evolution of CV of **1** and CV, DPV, and UV-vis of **2** upon addition of Mg^{2+} . UV-vis titration isotherm. B3LYP/3-21G*-optimized structures of **1** and **2** and complexation mode in **1**. ^1H NMR spectra for the titration of **1** and **2** with Mg^{2+} . This material is available free of charge via the Internet at <http://pubs.acs.org>.

OL050823Z

(13) Carr, J. D.; Coles, S. J.; Asan, M. B.; Hurthouse, M. B.; Malik, K. M. A.; Tucker, J. H. R. *J. Chem. Soc., Dalton Trans.* **1999**, 57.

(14) Connors, K. A. *Binding Constants: The Measurements of Molecular Complex Stability*; John Wiley & Sons Ltd.: New York, 1987; Chapter 4.